

E-Mail: editor.ijasem@gmail.com editor@ijasem.org

www.ijasem.org



# FAST DC-TYPE ELECTRIC VEHICLE CHARGER BASED ON A OUASI-DIRECT BOOST - BUCK RECTIFIER

# Dr. CHANDRASHEKHAR.M

Department of Electrical & Electronics Engineering, Annamacharya Institute of Technology and Sciences, Hyderabad, Telangana, India Shekharveltech453@gmail.com

# Mr. UPPU.NARESH

Department of Electrical & Electronics Engineering, Annamacharya Institute of Technology and Sciences, Hyderabad, Telangana, India unaresh52@@gmail.com

# Mr. THATIKONDA.KUMAR

Research Scholar,
Department of Electrical l&
Electronics Engineering,
Annamacharya Institute of
Technology and Sciences,
Hyderabad, Telangana,
IndiaKumarttt55@gmail.com

#### **ABSTRACT**

This work presents a DC-type fast electric vehicle battery charger featuring low switching losses. Herein, a conventional three-phase two-level voltage source rectifier with low capacitive energy storage operates with a discontinuous PWM modulation where each phase-legs stops switching for 240° of the grid fundamental period, i.e. only a single phase-leg switch every 60°. In this case, this AC-DC converter loses voltage controllability of the DC-link and thus a buck-type DC-DC converter is cascaded in order to provide the necessary voltage regulation and current limitation for the charging process of the electric vehicle. The presented circuit is benchmarked against other solutions for a designed 50 kW power capability battery charger when considering the charging of a 30 kWh Nissan Leaf. The results show a superior power efficiency of the studied system.

# I. INTRODUCTION

The electric vehicle (EV) charging market is very dynamic. Companies and institutes involved in the research and development of this area are devoted to considerably reduce the EV charging times to be close to the ones spent by users in gasstations filling the fuel of the internal combustion engines vehicles (ICEVs) [1]-[16]. Today most EVs can be charged at 50 kW and 400 V following the fast charging standards "CCS-up to 80kW" and "CHAdeMO – approx. 50kW". However new EVs are designed to withstand higher charging power. Therefore, output power scalability will be a key feature of the EV charging system by usage of power electronics building blocks (PEBB), i.e. the total power can be scalable by paralleling circuits. This leads to manufacturing advantages because a single circuit building block design can satisfy a plurality of business and many charging standards.

Connections to medium-voltage (MV) level AC grid becomes economically sensible for EV chargers with power capabilities of several 100 kW than today's most used 380V-480 V grid. In the power places where high charger installed,localenergystoragesystems,likebatterybanks, become more and more often used in order to mitigate power fluctuations and power quality issues of the AC grid. Local renewable energy generation systems may also be used to buffer the power demand and reduce energy consumption from the grid. In fact, there is a great potential for the use of photovoltaic (PV) energy generation as available surfaces in the roofs of the EV charging station and the nearby buildings can be greater than

1000 m<sup>2</sup>. Both batteries and PV systems can also be integrated into the charger itself as proposed in[7]-[8].

In Fig. 1 a suitable bidirectional PEBB circuit is shown for a high power DC-type EV charger with connection to a MV grid through a 50/60 Hz transformer. Advantageously, the battery charger can be fully assembled with half-bridge power modules, which has a large number of manufacturers with several current ratings and blocking voltage available.

By close inspection of the circuit depicted in Fig. 1., one can identify a well-known two-stage power conversion system, i.e. a three-phase AC-DC converter + a DC-DC circuit. The back-end circuit works as a three-channel PWM interleaved DC-DC buck-type converter. This features enhanced loss distribution among semiconductors or better current shared between the parallel circuits than hard-paralleling of semiconductors.

This results in improvements in the achievable total conduction and switching losses. Additionally, the symmetric PWM interleaved operation will cancel out the high frequency harmonics proportional to the number of employed parallel circuits in both voltages and currents, lowering the *rms* current across the DC capacitors Cf and Co. This feature can be used to enlarge the current ripple across each phase-leg of the back-end circuit in order to achieve Zero-Voltage-Switching turn-on of the active switches and low reverse-recovery losses of the anti-parallel diodes. The front-end converter comprises a three-phase three-wire two-level six-switch voltage source rectifier (2L-VSR), which inherent features low complexity and low cost. Note that with proper voltage conversion rate between the AC grid and EV battery the current stress across the front- and back-end circuits can be similar, which

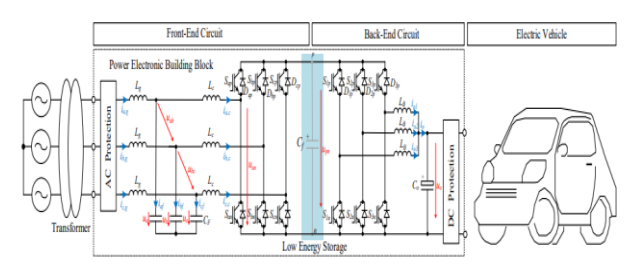
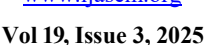


Fig. 1 proposed system

Fig.1 EV charger concept with back-end power conversion based on the PWM interleaved Buck-converter and front-end circuit based on the two-level bidirectional six-switch voltage source rectifier. Note that the systems are connected to





each other through a low energy storage DC-link will bring a manufacturing advantage.

In this paper, the front- and back-end circuits are intentionally connected through a DC-link employing capacitors with low energy storage capability, e.g. electrolytic capacitorless DC-link. This makes the operation of both circuits highly coupled to each other. The DC-link or voltage across the terminals p and n (or upn) in Fig. 1 will follow the rectified envelop of the AC capacitors line-to-line voltages, similarly to what is achieved by a basic three-phase diode-bridge rectifier. This allows that the rectifier phase-legs operate with a unique discontinuous PWM modulation (DPWM) where they can stop switching during two-thirds of the grid period or 240°, while the AC currents are at their highest values, i.e. only one phase-leg switch during every 60°. This operation was previously reported in [17] and it yield to the best switching loss reduction in any known DPWM strategy, e.g. the ones described in [20]-[21], but at the cost of losing voltage controllability of upn. The back-end circuit becomes necessary for voltage regulation and current limitation for the charging process of the EV batteries. Additionally, high power factor operation can only be achieved if the back-end converter ensures constant power operation. In [18] a VIENNA-type and in [19] a DELTA-SWITCH-type front-end circuit with similar operation have been proposed.

The goal of this paper is to analyse the benefits of implementing the DPWN with  $240^{\circ}$  stop switching interval in the widely used 2L-VSR considering the application of a fast EV battery charger.

The explanation of the structural characteristics of the presented DC-type EV charger, suitable modulation strategy featuring low switching losses and feedback control method, guaranteeing high-power-factor operation, are presented the analytical equations for calculating the power semiconductors and passives stresses with dependency on the AC or DC current amplitudes and the voltage transfer ratio of the converter are given. In Section V, the circuit in Fig. 1.1 is benchmarked against other suitable solutions for a 50 kW PEBB system regarding the achievable efficiency when considering the fast charging of a 30 kWh Nissan Leaf vehicle from state-of-charging (SoC) 0 % to 90%.

# II. THREE-PHASE EVBATTERY CHARGER

This section describes the basic operation of the EV battery charger depicted in Fig. 2 As previously discussed the front- and back-end circuits are connected to each other through a DC-link with low energy storage capability, which makes the operation of both circuits highly coupled to each other. In fact, the circuit operates similarly to a single- stage three-phase buck-type AC-DC converter [22]-[27], where the two largest AC line-to-line voltages are deliberately switched to the output of the back-end semiconductor bridge and a cascading low-pass filtering (LB and  $C_O$ ) in order to regulate the output voltage  $u_O$  used to charge the EV. Correspondingly, the output voltage can ideally be adjusted to values starting from zero to values.

$$u_o < \sqrt{\frac{3}{2}} u_{g,l-l,rms},$$

where,  $u_{g,l-l,rms}$  is the AC line-to-line rms voltage.

(1)

Note that the operation of the back-end circuit impressing (fundamental) constant power  $P_0$  will result in the demand of a current,  $I_X$ , varying in opposite phase to the six-pulse rectifier voltage at the output of the front-end circuit. During every  $60^{\circ}$  of the grid voltage, in the three-wire system sinusoidal shape of all AC grid phase currents, iabc,c, will be guaranteed by the overlaying of the circulating  $I_X$  with the current  $I_Y$  controlled by the switched phase-leg of the front- end circuit which has the lowest instant absolutevoltage.

For proof of the sinusoidal controllability of the grid currents, the equivalent circuit of the studied system for the grid interval  $[0^{\circ}, 30^{\circ}]$  or ua > ub > uc (c.f. Fig.3), which is depicted in Fig. 3, is considered for analysis. Ideally, no fundamental frequency voltage drop across the AC inductorsoccurs and the EV system operates as a symmetric three-phase load of phase conductance G to the grid,

$$u_{Lc} = 0, (2)$$

Therefore, the value of the current to be controlled at phase b may be written as

$$\overline{I}_{y} = -i_{b,c} = -Gu_{b}. \tag{3}$$

DC Fast Charging bypasses all of the limitations of the on-board charger and required conversion, instead providing DC power directly to the battery, charging speed has the potential to be greatly increased. Charging times are dependent on the battery size and the output of the dispenser, and other factors, but many vehicles are capable of getting an 80% charge in about or under an hour using most currently available DC fast chargers.

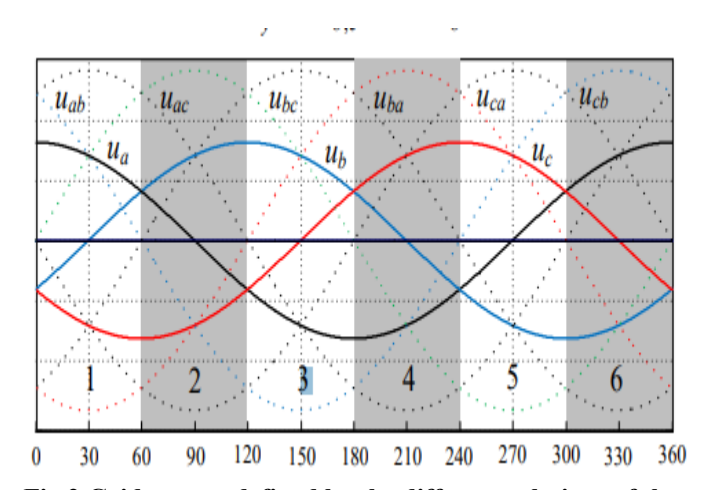


Fig.2 Grid sectors defined by the different relations of the instantaneous values of the grid phase voltages ua,b,c



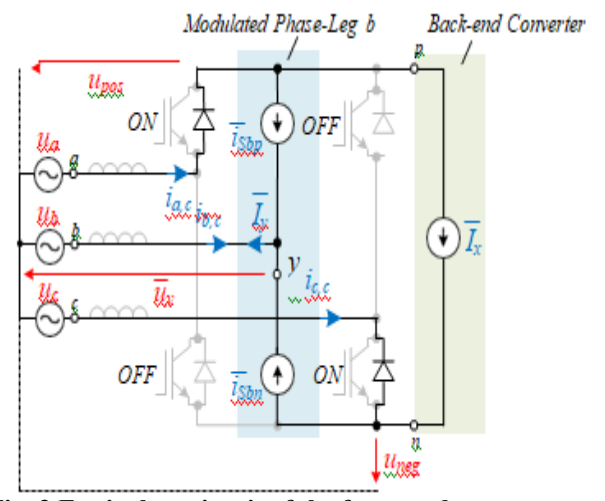


Fig. 3 Equivalent circuit of the front-end convert operation for ua>ub>uc

# A. DC Fast Charging Explained

AC charging is the simplest kind of charging to find – outlets are everywhere and almost all EV chargers you encounter at homes, shopping plazas, and workplaces are Level 2 AC chargers. An AC charger provides power to the on-board charger of the vehicle, converting that AC power to DC in order to enter the battery. The acceptance rate of the on-board charger varies by brand but is limited for reasons of cost, space and weight. This means that depending on your vehicle it can take anywhere from four or five hours to over twelve hours to fully charge at Level 2.

DC Fast Charging bypasses all of the limitations of the on-board charger and required conversion, instead providing DC power directly to the battery, charging speed has the potential to be greatly increased. Charging times are dependent on the battery size and the output of the dispenser, and other factors, but many vehicles are capable of getting an 80% charge in about or under an hour using most currently available DC fast chargers.

DC fast charging is essential for high mileage/long distance driving and large fleets. The quick turnaround enables drivers to recharge during their day or on a small break as opposed to being plugged in overnight, or for many hours, for a full charge.

Older vehicles had limitations that only allowed them to charge at 50kW on DC units (if they were able to at all) but newer vehicles are now coming out that can accept up to 270kW. Because battery size has increased significantly since the first EVs hit the market, DC chargers have been getting progressively higher outputs to match – with some now being capable of up to 350kW.

Currently, in North America there are three types of DC fast charging: CHAdeMO, Combined Charging System (CCS) and Tesla Supercharger.

All major DC charger manufacturers offer multistandard units that offer the ability to charge via CCS or CHAdeMO from the same unit. The Tesla Supercharger can only service Tesla vehicles; however Tesla vehicles are capable of using other chargers, specifically CHAdeMO for DC fast charging, via an adapter.

Some types of fast charging only work with specific cables and chargers. It is also important to reiterate the fact the technology works either through higher current flows or higher

voltage. What these mean is that the general fast charging technology has compatibility issues. A particular adaptive charger from Samsung will not effectively charge an iPhone capable of fast charge. Chargers for VOOC Flash Charging would not work with the Quick Charge from Qualcomm Accordingly, the fundamental voltage formed at the input of the bridge-leg will be given by

$$\overline{u}_{v} = u_{b}. \tag{4}$$

If the voltage at the terminal y is formed according to the relative on-time of the transistor Sbpas kyand Sbnas (1-ky), it will result in

$$\overline{u}_{y} = k_{y} \cdot u_{a} + (1 - k_{y}) \cdot u_{c} = k_{y} \cdot u_{ac} + u_{c}. \tag{5}$$

For the switch on-time ky given by

$$k_{y} = \frac{-u_{pos} - 2u_{neg}}{u_{pos} - u_{neg}} = \frac{u_{bc}}{u_{ac}},$$
 (6)

Where

$$u_{pos} = \max(u_a, u_b, u_c)$$
 and  $u_{neg} = \min(u_a, u_b, u_c)$ , (7)

$$\overline{i}_{Sbp} = k_y \cdot \overline{I}_y = -k_y \cdot i_{b,c} = -k_y \cdot G \cdot u_b = -G \cdot u_b \cdot \frac{u_{bc}}{u_{ac}}.$$
 (8)

Considering the fundamental input currents that have to be generated at the input

Three-phase electrical power was developed in the 1880s by multiple people. Three-phase power works by the voltage and currents being 120 degrees out of phase on the three wires. As an AC system it allows the voltages to be easily stepped up using transformers to high voltage for transmission, and back down for distribution, giving high efficiency.

Three-phase electric power (abbreviated  $3\phi$ ) is a common type of alternating current used in electricity generation, transmission, and distribution. It is a type of polyphase system employing three wires (or four including an optional neutral return wire) and is the most common method used by electrical grids worldwide to transfer power.

$$i_{a,c} = G \cdot u_a$$
,  $i_{b,c} = G \cdot u_b$  and  $i_{c,c} = G \cdot u_c$ , (9)

$$\overline{I}_x = k_x \frac{P_o}{u} \tag{10}$$

$$k_{x} = \frac{u_{o}}{u_{nos} - u_{neo}} \tag{11}$$

gives

$$\overline{I}_{x} = \frac{P_{o}}{u_{ac}} = \frac{i_{a,c} \cdot u_{ac} + i_{b,c} \cdot u_{bc}}{u_{ac}} = G \cdot \frac{u_{a} \cdot u_{ac} + u_{b} \cdot u_{bc}}{u_{ac}}.$$
 (12)

The resultant fundamental frequency current drawn from phase a is proportional to its phase voltage

$$i_{a,c} = \overline{I}_x + \overline{i}_{Sbp} = G \cdot u_a \,. \tag{13}$$

Additionally, the fundamental frequency current for phase c can be determined using (3), (12), and the main three-wire system expressions



$$i_{a,c} + i_{b,c} + i_{c,c} = 0$$
, and  $u_a + u_b + u_c = 0$  (14)

yielding to

$$i_{c,c} = \overline{i}_{Sbn} - \overline{I}_x = (1 - k_y) \cdot \overline{I}_y - \overline{I}_x = G \cdot u_c.$$
 (15)

Therefore, sinusoidal shape of all AC phase currents has been proven for the grid interval [0°, 30°].

Finally, high power factor operation and controlled output voltage,  $u_0$ , for all grid sectors can be achieved if the single switched phase-leg of the front-end circuit, i.e. the one with the lowest instant absolute voltage, is modulated with a relative on-time ky (c.f. Eq. (6)), together with the back-end circuit constantly modulated with the on-time k(c.f. Eq. (11)). Those variable are dependent on the instantaneous values of the AC grid voltages  $u_a$ , b, c and the output voltage  $u_0$  (cf. Table I). B. Three-Phase Electric Power

Three-phase electric power (abbreviated  $3\phi$ ) is a common type of alternating current used in electricity generation, transmission, and distribution. It is a type of polyphase system employing three wires (or four including an optional neutral return wire) and is the most common method used by electrical grids worldwide to transfer power.

Three-phase electrical power was developed in the 1880s by multiple people. Three-phase power works by the voltage and currents being 120 degrees out of phase on the three wires. As an AC system it allows the voltages to be easily stepped up using transformers to high voltage for transmission, and back down for distribution, giving high efficiency.

A three-wire three-phase circuit is usually more economical than an equivalent two-wire single-phase circuit at the same line to ground voltage because it uses less conductor material to transmit a given amount of electrical power. Three-phase power is mainly used directly to power large induction motors, other electric motors, and other heavy loads. Small loads often use only a two-wire single-phase circuit, which may be derived from a three-phase system.

# A. Principle

Normalized waveforms of the instantaneous voltages in a threephase system in one cycle with time increasing to the right. The phase order is 1-2-3. This cycle repeats with the frequency of the power system. Ideally, each phase's voltage, current, and power is offset from the others' by 120°.

In a symmetric three-phase power supply system, three conductors each carry an alternating current of the same frequency and voltage amplitude relative to a common reference, but with a phase difference of one third of a cycle (i.e. 120 degrees out of phase) between each. The common reference is usually connected to ground and often to a current-carrying conductor called the neutral. Due to the phase difference, the voltage on any conductor reaches its peak at one third of a cycle after one of the other conductors and one third of a cycle before the remaining conductor. This phase delay gives constant power transfer to a balanced linear load. It also makes it possible to produce a rotating magnetic field in an electric motor and generate other phase arrangements using transformers (for instance, a two phase system using a Scott-T transformer). The amplitude of the voltage difference between two phases is {\displaystyle {\sqrt {3}}} $\sqrt{3}$  (1.732...) times the amplitude of the voltage of the individual phases.

The symmetric three-phase systems described here are simply referred to as three-phase systems because, although it is possible to design and implement asymmetric three-phase power systems (i.e., with unequal voltages or phase shifts), they are not used in practice because they lack the most important advantages of symmetric systems.

In a three-phase system feeding a balanced and linear load, the sum of the instantaneous currents of the three conductors is zero. In other words, the current in each conductor is equal in magnitude to the sum of the currents in the other two, but with the opposite sign. The return path for the current in any phase conductor is the other two phase conductors.

Constant power transfer and cancelling phase currents are possible with any number (greater than one) of phases, maintaining the capacity-to-conductor material ratio that is twice that of single-phase power. However, two phases results in a less smooth (pulsating) current to the load (making smooth power transfer a challenge), and more than three phases complicates infrastructure unnecessarily.

Three-phase systems may have a fourth wire, common in low-voltage distribution. This is the neutral wire. The neutral allows three separate single-phase supplies to be provided at a constant voltage and is commonly used for supplying multiple single-phase loads. The connections are arranged so that, as far as possible in each group, equal power is drawn from each phase. Further up the distribution system, the currents are usually well balanced. Transformers may be wired to have a four-wire secondary and a three-wire primary, while allowing unbalanced loads and the associated secondary-side neutral currents.

# B. Phase sequence

Wiring for the three phases is typically identified by colors which vary by country. The phases must be connected in the right order to achieve the intended direction of rotation of three-phase motors. For example, pumps and fans do not work in reverse. Maintaining the identity of phases is required if two sources could be connected at the same time; a direct interconnect between two different phases is a short circuit.

# III. CONTROL STRATEGY AND PWMMODULATION

A possible implementation of a feedback control and PWM modulation strategy for the studied EV charging system is shown in Fig.4The AC currents are controlled in the  $\alpha$ - $\beta$  coordinates, where the variables  $\alpha$ - $\beta$  components are obtained with the Clarke transformation given by

$$\begin{bmatrix} i_{\alpha} \\ i_{\beta} \end{bmatrix} = \frac{2}{3} \begin{bmatrix} 1 & -1/2 & -1/2 \\ 0 & \sqrt{3}/2 & -\sqrt{3}/2 \end{bmatrix} \begin{bmatrix} i_{a,c} \\ i_{b,c} \\ i_{c,c} \end{bmatrix}.$$
 (16)

This control scheme includes an outer DC voltage loop for uowhich, together with the information of the AC voltages in  $\alpha$ - $\beta$ , generates the AC current references  $i\alpha$ ,  $\beta^*$ . This voltage loop control also set the reference for the partial currents io,  $n^*$  across the parallel Buck-converters. Herein, a phase-locked-loop (PLL) circuit is used in order to determine the instantaneous phase angle wgt from the grid line-to-line voltage measurements, uab and ubc. The modulation functions ensuring high-power-factor operation, ma, mb, mc and mBuck, are synthesized from the six AC voltage sectors and the  $\alpha$ - $\beta$  components of the duty-



cycle functions  $d\alpha$  and  $d\beta$  transformed back to abc coordinates in line-to-line quantities, uab\*/ubc\*/uca\*/uba\*/ucb\*/uac\*, as described in TableI.

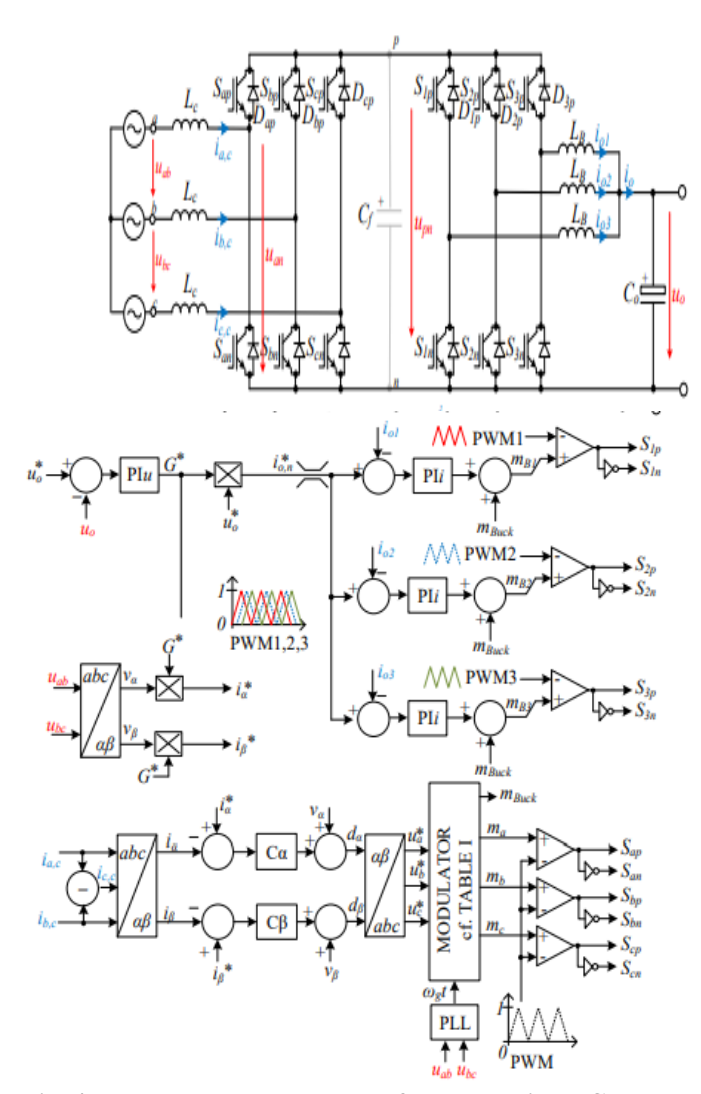


Fig. 4 Feedback control strategy for the studied DC-type EV charger

Herein, uo \* is the output voltage reference, which must satisfy Eq. (1).

# A. PID Controller Design

PID (proportional integral derivative) control is one of the earlier control strategies. Its early implementation was in pneumatic devices, followed by vacuum and solid state analog electronics, before arriving at today's digital implementation of microprocessors. It has a simple control structure which was understood by plant operators and which they found relatively easy to tune. Since many control systems using PID control have proved satisfactory, it still has a wide range of applications in industrial control. According to a survey for process control systems conducted in 1989, more than 90 of the control loops were of the PID type. PID control has been an active research topic for many years; see the monographs. Since many process plants controlled by PID controllers have similar dynamics it has been found possible to set satisfactory controller parameters from less plant information than a complete mathematical model. These techniques came about because of the desire to adjust controller parameters in situ with a minimum of effort, and also because of the possible difficulty and poor cost benefit of obtaining mathematical models.

TABLE I
Main modulation functions for the EV charger

					<u></u>
Sector	$k_y$	$k_x/m_{buck}$	$m_a$	$m_b$	$m_c$
I: 0°-60°	$u_{bc}^*/u_{ac}^*$	$u_o^*/u_{ac}^*$	1 or 0	$k_y$	0
II: 60°-120°	$u_{ac}^*/u_{bc}^*$	$u_o^*/u_{bc}^*$	$k_y$	1 or 0	0
III: 120°-180°	$u_{ca}^*/u_{ba}^*$	$u_o^*/u_{ba}^*$	0	1 or 0	$k_{v}$
IV: 180°-240°	$u_{ba}^*/u_{ca}^*$	$u_o^*/u_{ca}^*$	0	$k_y$	1 or 0
V: 240°-300°	$u_{ab}^*/u_{cb}^*$	$u_o^*/u_{cb}^*$	$k_y$	0	1 or 0
VI: 300°-360°	$u_{cb}^*/u_{ab}^*$	$u_o^*/u_{ab}^*$	1 or 0	0	$k_y$

The two most popular PID techniques were the step reaction curve experiment, and a closed-loop "cycling" experiment under proportional control around the nominal operating point. In this chapter, several useful PID-type controller design techniques will be presented, implementation issues for the algorithms will also be discussed. The proportional, integral, and derivative actions are explained in detail, and some variations of the typical PID structure are also introduced. In the well-known empirical Ziegler- Nichols tuning formula and modified versions will be covered. Approaches for identifying the equivalent first-order plus dead time model, which is essential in some of the PID controller design algorithms, will be presented. A modified Ziegler-Nichols algorithm is also given. Some other simple PID setting formulae such as the Chien-Hrones-Reswick formula, Cohen-Coon formula, refined Ziegler-Nichols tuning, Wang-Juang-Chan formula and Zhuang-Atherton optimum PID controller will be presented in Sec. 6.3. In Sec. 6.4, the PID tuning formulae for FOIPDT (first- order lag and integrator plus dead time) and IPDT (integrator plus dead time) plant models, rather than the FOPDT (first-order plus dead time) model.

# IV. SIMULATION RESULTS

Fig. 5 and Fig. 6 show the main waveforms of the studied EV battery charger obtained in a circuit simulator. Therein, the converter specification listed in Table II is considered. Fig. 4.1 presents the main waveforms generated by the modulation functions described in Table I. As it can be observed in Fig. 6, the results demonstrate that the converter-side AC currents ia,c, ib,c, and ic,c, can effectively follow the sinusoidal input phase voltages ua,b,c, while the current across the parallel Buckconverters are well balanced, attesting the feasibility of the studied PEBB circuit and control method depicted in Fig. 4. Fig. 6(c) shows the converter voltage across the AC terminal in phase a and the terminal n of the DC-link attesting that the bridgeleg can stop switching for two-thirds of the grid period without impairing the high-power-factor operation. In order to verify the accuracy of the derived equations modeling the current stresses of the system components, an appropriate switching frequency and the values of the passive components according to (30), (33), (35) and (36) have been selected. A switching frequency of fs = 16 kHz is designated as it constitutes a good compromise between high efficiency, high power density, and high control bandwidth. The values of the main components are listed in Table II. In Table III, the values of the component stresses calculated with the respective equations are compared to the results obtained with a digital simulation and show a good accuracy



Table II. Electrical vehicle fast DC-type charger specifications

Rated output power $P_o$	50 kW		
Input phase voltage $u_{a,rms}$	230 V (RMS)		
Output voltage $u_0$	400 V		
Grid $f_g$ and switching frequencies $f_s$	50 Hz / 16 kHz		
LCL ac filter $L_g/L_c/C_F$	100.0 μΗ/200.0 μΗ/20.0 μF		
Buck-converter Inductor $L_B$	300.0 μΗ		
Partial DC capacitors $C_f$	25.0 μF		
Output capacitor $C_o$	200 μF		

Table III Comparison of active and passive component stresses determined by analytical calculations and digital simulations

	Analytical Calculations	Simulation	Deviation [%]
$I_{Sabc,avg}$	0.79	0.80	-1.25
$I_{Sabc,rms}$	4.60	4.62	-0.43
$I_{Dabc,avg}$	31.75	31.83	-0.25
$I_{Dabc,rms}$	51.03	51.04	-0.02
$I_{S123p,avg}$	31.04	31.03	+0.03
$I_{S123p,rms}$	35.96	36.00	-0.11
$I_{D123n,avg}$	10.63	10.63	+0.00
$I_{D123n,rms}$	21.05	21.06	-0.05
$\Delta i_{LB,pp,max}$	24.17	24.13	+0.16
$\Delta i_{Lc,pp,max}$	29.343	30.00	-2.2
$\Delta u_{Co,pp,max}$	0.105	0.106	-0.94
$\Delta u_{Cf,pp,max}$	64.34	65.00	-1.01

The two most popular PID techniques were the step reaction curve experiment, and a closed-loop "cycling" experiment under proportional control around the nominal operating point. In this chapter, several useful PID-type controller design techniques will be presented, and implementation issues for the algorithms will also be discussed. The proportional, integral, and derivative actions are explained in detail, and some variations of the typical PID structure are also introduced. In the well-known empirical Ziegler- Nichols tuning formula and modified versions will be covered.

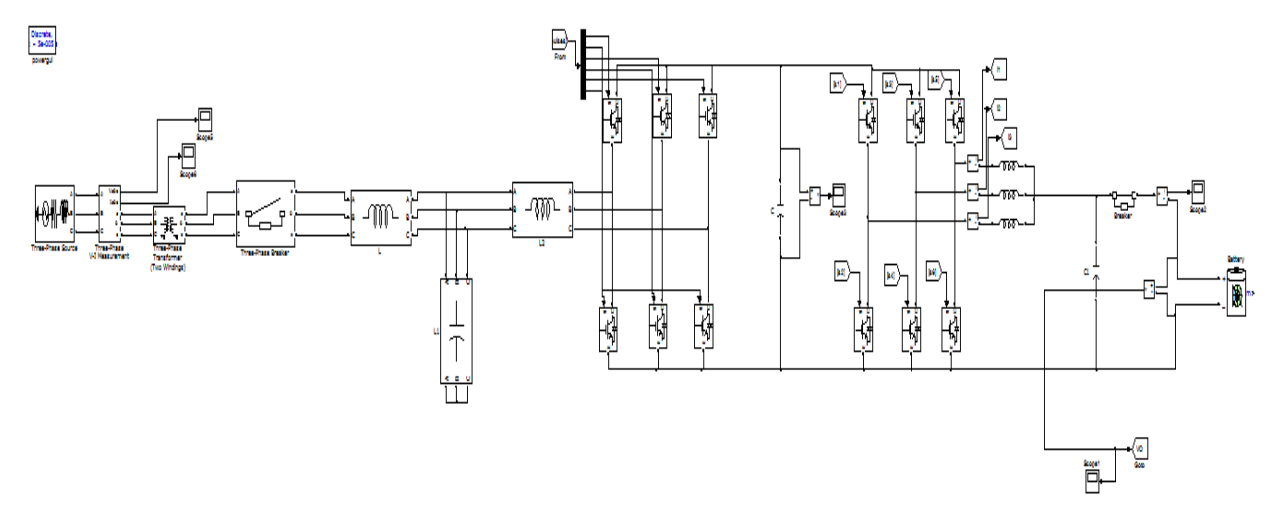


Fig. 5 Proposed system circuit configuration



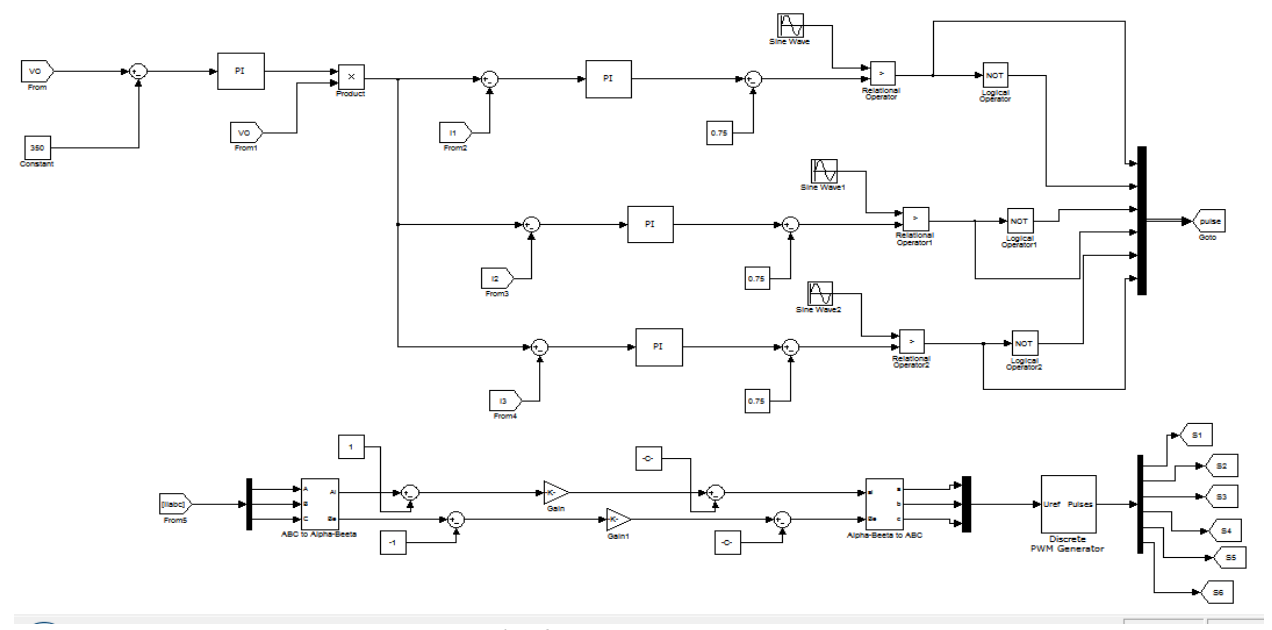


Fig. 6 Proposed controllers

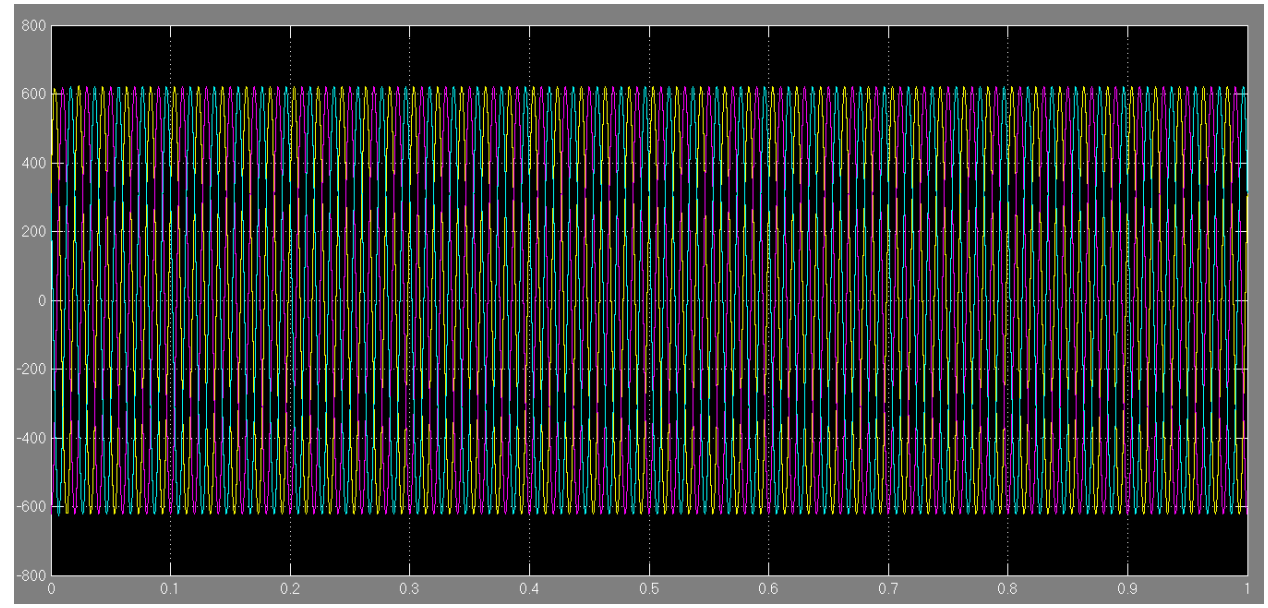


Fig. 7 Input voltage for proposed system



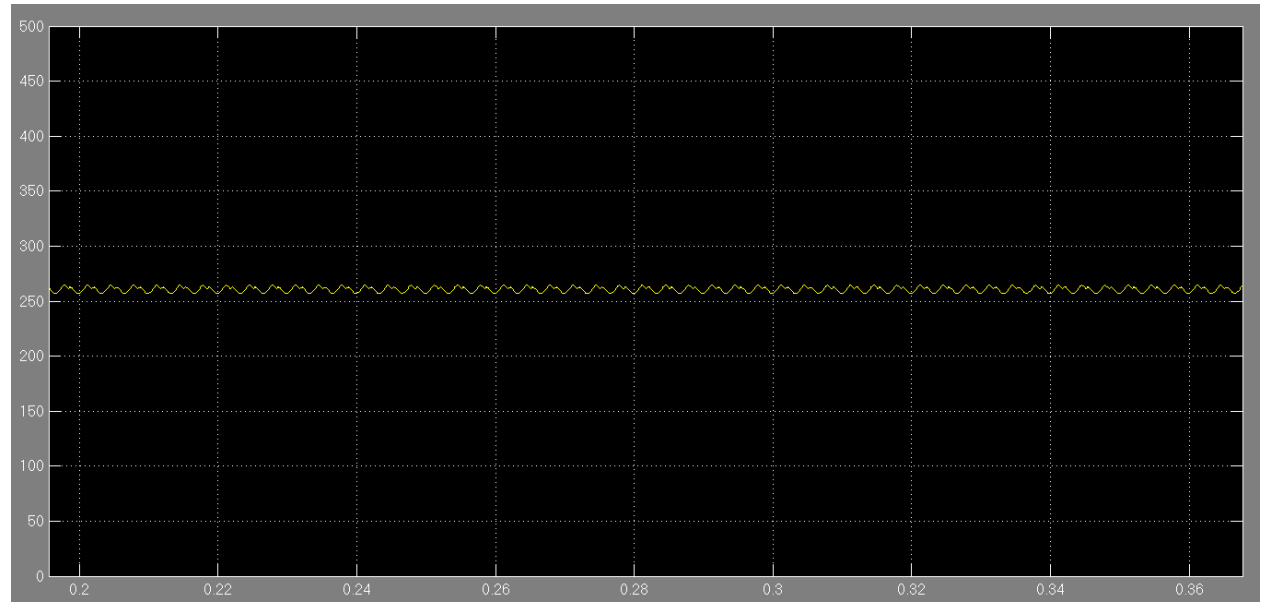


Fig .8 DC-link voltages for proposed system

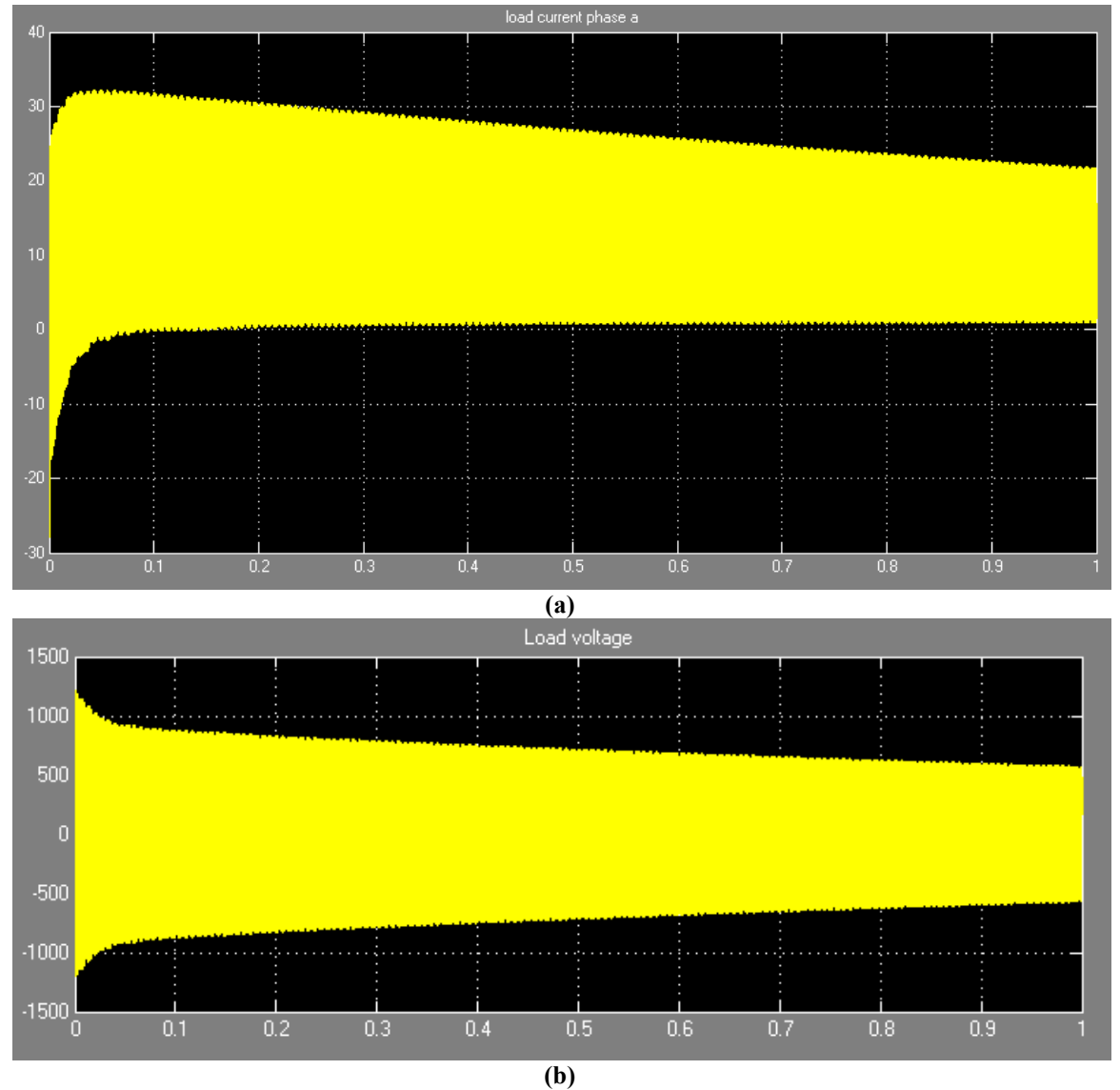


Fig.9 load voltage and load current



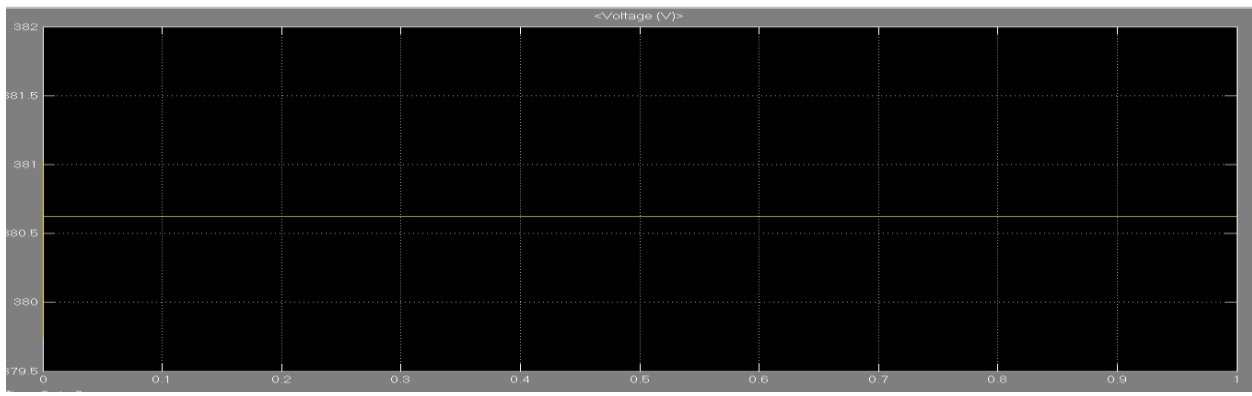


Fig. 10 Battery voltage

Fig. 7 and Fig. 8 show the main waveforms of the studied EV battery charger obtained in a circuit simulator. Therein, the converter specification listed in Table II is considered. Fig. 4.5 presents the main waveforms generated by the modulation functions described in Table I. As it can be observed in Fig. 4.6, the results demonstrate that the converter-side AC currents ia, c, ib,c, and ic,c, can effectively follow the sinusoidal input phase voltages ua,b,c, while the current across the parallel Buckconverters are well balanced, attesting the feasibility of the studied PEBB circuit and control method depicted in Fig. 4. Fig. 6(c) shows the converter voltage across the AC terminal in phase a and the terminal n of the DC-link attesting that the bridge- leg can stop switching for two-thirds of the grid period without impairing the high-power-factor operation order to verify the accuracy of the derived equations modeling the current stresses of the system components, an appropriate switching frequency and the values of the passive components according to (30), (35)and(36) havebeenselected. As witching frequency of f=16kHz is designated as it constitutes a good compromise between high efficiency, high power density, and high control bandwidth. The values of the main components are listed in Table II. In Table III, the values of the component stresses calculated with the respective equations are compared to the results obtained with a digital simulation and show agood accuracy.

# V. CONCLUSION AND FUTURE SCOPES

The three-phase DC-type electric vehicle battery concept employing a back-end power conversion based on the PWM interleaved Buck-converter and front-end circuit based on the two-level bidirectional six-switch voltage source rectifier has been studied. The implementation of a unique DPWM modulation was explained. This ensures high-power-factor operation while the phase-leg can stop switching during two-thirds of the grid period or 240°, reducing considerably the semiconductor switching losses. The principle of operation, the main designing expressions, suitable modulation scheme and PWM control have been described in theprofect. 20 30 40

A benchmark was presented for the merit of semiconductor power loss achieved for a 0 to 90% charging session of a Nissan Leaf car. Therein, a 50 kW DC-type EV charger is designed considering commercially available Wolf speed SiC MOSFET and Infineon Si IGBT power modules and suitable air cooling system. The analysis also considers the operation of the grid-connected power conversion with the studied DPWM240 and other well- stablished modulations, namely SVPWM and DPWM120. As expected, the calculations

show a superior performance in loss reduction and energy savings, for the DPWM240.

#### **FUTURE SCOPE**

Level 3 stations can bring some of the latest EVs up to an 80 percent charge in as little as 20-30 minutes. Experts

project there will be 35 million EVs will be on the road by 2030 and even with most only requiring an occasional hookup, the need for public chargers in the coming years will swell exponentially.

# REFERENCES

- [1] Dale Hall and NicLutsey, "Emerging best practices for electric vehicle charging infrastructure," in Proc. of the international council on clean transportation (ICCT), Oct.2017.
- [2] J. C. Spoelstra and J. Helmus, "Public charging infrastructure use in the Netherlands: a rollout-strategy assessment," in Proc. of European Battery, Hybrid and Fuel Cell Electric Vehicle Congress, Dec.2016.
- [3] Kuperman, U. Levy, J. Goren, A. Zafransky and A. Savernin "Battery charger for electic vehicle traction battery switch station," IEEE Trans. Ind. Electr., 2013. G. R. Chandra Mouli, M. Kefayati, R. Baldick, and P. Bauer, "Integrated pv charging of ev fleet based on dynamic prices, v2g and offer of reserves," IEEE Trans. Smart Grids, 2018.
- [4] M. Kesler, M. C. Kisacikoglu, and L. M. Tolbert, "Vehicle-to-grid reactive power operation using plugin electric vehicle bidirectional offboard charger," IEEE Trans. Ind. Electr.,2014.
- [5] J. C. Gomez and M. M. Morcos, "Impact of ev battery chargers on the power quality of distribution systems," IEEE Power Delivery, 2003.
- [6] S. Rahman and G. B. Shrestha, "An investigation into the impact of electric vehicle load on the electric utility distribution system," IEEE Trans. Power Delivery, 1993.
- [7] E. Sortomme and M. A. El-Sharkawi, "Optimal combined bidding of vehicle-to-grid ancillary services," IEEE Trans. Smart Grid,2012.
- [8] C. C. Chan and K. T. Chau, "An overview of power electronics in electric vehicles," IEEE Trans. Ind. Electr., 1997.
- [9] J. Sallan, J. L. Villa, A. Llombart and J. F. Sanz,



- "Optimal design of icpt systems applied to electric vehicle battery charge," IEEE Trans. Ind. Electr., 2009.
- [10] M. Vasiladiotis and A. Rufer, "A modular multiport power electronic transformer with integrated split battery energy storage for versatile ultrafast ev charging stations," IEEE Trans. Ind. Electr., 2015.
- [11] S. Bai and S. M. Lukic, "Unified active filter and energy storage system for an mv electric vehicle charging station," IEEE Trans. Power Electr., 2013.
- [12] C. Jiang, R. Torquato, D. Salles and W. Xu, "Method to assess the power quality impact of plug-in electric vehicles," IEEE Trans. Power Delivery, 2014.
- [13] D. Menzi, D. Bortis, and J. W. Kolar, "Three-phase two-phase- clamped boost-buck unity power factor rectifier employing novel variable dc link voltage input current control," Proc. of 2nd IEEE International Power Electronics and Application Conference and Exposition (PEAC) Nov. 4-7, 2018.
- [14] J. A. Anderson, M. Haider, D. Bortis, J. W. Kolar, M. Kasper, and G. Deboy, "New Synergetic Control of a 20 kW Isolated Vienna Rectifier Front-End EV Battery Charger," Proc. of 20th IEEE Workshop on Control and Modeling for Power Electronics (COMPEL) June 17-20,2019.
- [15] T. B. Soeiro, and P. Bauer, "Three-phase unidirectional quasi-single- stage delta-switch rectifier + dc-dc buck converter," in Proc. of 39th Ann. Conf. of the Ind.Electr. Soc., (IECON),2019.
- [16] AhmetMasumHava, "Carrier based pwm-vsi drives in the overmodulation region." PhD thesis,1998.
- [17] M. Hava, R. J. Kerkman, and T. A. Lipo. "A high performance generalized discontinuous pwm algorithm." IEEE Trans. Ind. Appl., pages 1059– 1071,1998.
- [18] L. Schrittwieser, J. W. Kolar and T. B. Soeiro, "99% efficient three- phase buck-type SiC MOSFET PFC rectifier minimizing life cycle cost in DC data centers," in Proc. *Intern. Telecommunications Energy Conference (INTELEC)*, Austin, TX, 2016, pp.1-8.
- [19] T. B. Soeiro, M. Ortmann and M. L. Heldwein, "Three-phase five- level bidirectional buck- + boosttype PFC converter for DC distribution systems," 2013 IEEE International Conference on Industrial Technology (ICIT), Cape Town, 2013, pp.928-933.
- [20] L. K. Ries, T. B. Soeiro, M. S. Ortmann and M. L. Heldwein, "Analysis of carrier-based pwm patterns for a three-phase five-level bidirectional buck + boost-type rectifier," in *IEEE Transactions on Power Electronics*, vol. 32, no. 8, pp. 6005-6017, Aug.2017.
- [21] T. B. Soeiro, M. L. Heldwein and J. W. Kolar, "Threephase modular multilevel current source rectifiers for electric vehicle battery charging systems," in Proc. of Brazilian Power Electronics Conference (COBEP),2013.
- [22] T. B. Soeiro, G. J. M. de Sousa, M. S. Ortmann and M. L. Heldwein, "Three-phase unidirectional buck-type third harmonic Injection Rectifier Concepts," in Proc. of 29th Ann. IEEE Appl. Power Electron. Conf. and Exp. (APEC),2014.
- [23] T. B. Soeiro, G. J. Maia, M. S. Ortmann and M. L. Heldwein, "High efficiency three-phase unidirectional buck type PFC rectifier concepts," in Proc. of 39th

Annual Conference of the Industrial Electronics Society, IECON2013.

[24] https://fastned.nl/nl/blog/post/everything-you-ve-always-wanted-to-know-about-fast-charging.

#### **Author Profile:**



**Dr. CHANDRA SHEKHAR .M** has Assistant Professor in ELECTRICAL AND ELECTRONICS ENGINEERING at ANNAMACHARYA INSTITUTE OF TECHNOLOGY & SCIENCES, Hyderabad, India .Has 14 years of teaching experience in engineering colleges He has received his Ph.D. in Electrical Engineering From VELTECH University in 2025 and M.Tech in power Electronics from AURORAS Engineering college in 2012 and B.Tech in Electrical and Electronics Engineering from PRRM Engineering college in 2005.

Areas of interests are WOT (WEB of things), Artificial Intelligence, Cloud computing, Power Electronics, Control Systems, power systems and Electrical machines.

EMAIL ID: shekharveltech453@gmail.com



UPPU.NARESH has Assistant Professor in ELECTRICAL AND ELECTRONICS ENGINEERING at ANNAMACHARYA INSTITUTE OF TECHNOLOGY& SCIENCES, Hyderabad, India .Has 9 years of teaching experience in engineering colleges He has M.Tech in power Electronics and electric drives from Arjun college of Engineering & Technology in 2014 and B.Tech in Electrical and Electronics Engineering from Siddhartha institute of Engineering & Technology in 2012.

Areas of interests are WOT (WEB of things), FIOT, Cloud computing, Power Electronics, Control Systems, power systems and Electrical machines, Basic electrical and engineering.

EMAIL ID: unaresh52@gmail.com





# **SCHOLAR DETAILS:**



Mr. Thatikonda Kumar. Completed B-Tech in **SREE** DATTHA INSTITUTE OF ENGINEERING AND SCIENCE at 2015 now he is pursuing M.Tech in ANNAMACHARYA TECHNOLOGY INSTITUTE OF SCIENCE

EMAILID: <u>kumarttt55@gmail.com.</u>